 doi:10.20944/preprints202205.0336.v1

Article

LncRNA prostate androgen-regulated transcript 1 (PART-1) promotes the non-small-cell lung cancer progression via regulating miR-204-3p/IGFBP-2 pathway

Kenfen Li [1], Yanping Zhang [1], Yunfeng Wang[2], Xin Guo [1], Xianhui Dai[1], and Li Song [3,*]

[1]Department of Respiratory and Critical Care Medicine, People's Hospital of ChengYang District, Shandong First Medical University, Qingdao, 266109, China; lkf1611@163.com (K.F.L.); 983233819@qq.com (Y.P.Z.); 1028532964@qq.com (X.G.); daixianhui1976@126.com (X.H.D)

[2] Department of Clinical Laboratory, People's Hospital of ChengYang District, Shandong First Medical University, Qingdao, 266109, China; wangyunfeng1351@126.com

[3]Department of Respiratory Medicine, Shanghai Eighth People's Hospital, Shanghai 200233, China; 147150379@qq.com

* Correspondence: 147150379@qq.com;

Abstract: Lung cancer is a common malignant tumor of the lung and the leading cause of cancer mortality worldwide. Non-small-cell lung cancer (NSCLC) accounts for 80%–85% of lung cancer, 40% of NSCLCs will have spread beyond the lungs by the time it is diagnosed. Long non-coding RNA (LncRNA) prostate androgen-regulated transcript 1 (PART-1) was reported that promote the development of several cancers. In the current study, we conducted experiments to investigate the role of PART-1 in the proliferation, invasion, and migration of NSCLC. The expression level of the PART-1 gene increased significantly in the NSCLC cell lines, including A549, H1229, H1650, H1975, and PC9. Knocking down of PART-1 inhibited the proliferation, invasion, and migration of A549 cells, moreover, decreased the tumor proliferation in nude mice. We confirmed that PART-1 targeted miR-204-3p directly, and miR-204-3p targeted the insulin-like growth factor binding protein 2 (IGFBP-2) directly. Furthermore, we discovered that PART-1 involved the NSCLC progression by regulating the miR-204-3p-targeted IGFBP-2 pathway. LncRNA PART-1 might be a target for treating NSCLC, and a warning sign of diagnosis of early lung cancer.

Keywords: keyword 1; Long non-coding RNA; Prostate androgen-regulated transcript 1; miR-204-3p; insulin-like growth factor binding protein 2

1. Introduction

Lung cancer is a common malignant tumor of the lung and the leading cause of cancer-related death [1]. Most lung cancers are diagnosed at an advanced stage because of no clinical symptoms or effective screening programs [1]. The incidence of lung cancer in the world has been on the rise, and lung cancer is the leading cause of cancer mortality worldwide [2]. Although disease understanding, treatment options, and outcomes for lung cancer are improving, 5-year survival continue to be low [3]. Lung cancer could be divided into small cell lung cancer (SCLC) and non-small-cell lung cancer (NSCLC) according to the histopathological characteristics [4]. NSCLC accounts for 80%–85% of lung cancer, and each type of NSCLC has different kinds of cancer cells, which grow and spread in different ways [5]. Although a large number of different markers have been proposed to predict the risk of NSCLC progression, few of them are used in clinical practice [5].

Long non-coding RNAs (lncRNAs) are defined as transcripts greater than 200 nucleotides, transcribed by RNA polymerase II, but not translated into proteins [6]. LncRNAs participate in multiple biological processes and are closely related to human diseases though their role is still largely unknown [7]. LncRNAs can regulate mRNAs through shared microRNAs and plays critical roles in the development of tumor via acting as

Preprints (www.preprints.org) | NOT PEER-REVIEWED | Posted: 24 May 2022 doi:10.20944/preprints202205.0336.v1

competing endogenous RNAs (ceRNAs) [8]. LncRNA prostate androgen-regulated transcript 1 (PART-1) has been reported as a tumor oncogene [9]. PART-1 serves as a competing endogenous RNA to promote Osteosarcoma (OS) tumorigenesis via its regulation of the miR-20b-5p/BAMBI axis [10]. In addition, PART-1 regulated colorectal cancer via activation of the Wnt/beta-catenin pathway and regulation of miR-150-5p/miR-520h/CTNNB1 [11]. However, the mechanisms underlying PART-1 involvement in NSCLC are still unclear.

MicroRNAs (miRNAs) are endogenous non-coding RNAs that negatively regulate the expression of downstream targeted mRNAs via binding with the 3′-untranslated region (UTR) of targets [12]. MiRNAs act as tumor suppressors or oncogenes to interfere with the progression of cancers including cell proliferation, differentiation, and apoptosis [13,14]. MiRNA MiR-204-3p was reported to function in the potential tumor suppressive in cancers. The down-regulated of miR-204-3p increased the expression of fibronectin 1 and promoted the invasion of clear cell renal cell carcinoma (ccRCC) cells [15]. Down-regulation of miR-204-3p was correlated with lymph node metastasis and larger tumor size, however, overexpression of miR-204-3p significantly suppressed the proliferation and induced apoptosis of Bladder cancer (BC) cells [16]. The insulin-like growth factor binding protein 2 (IGFBP-2) was validated as a direct target gene of miR-204-3p [17], which is a potential biomarker for diagnosis of severe malnutrition in patients with advanced lung cancer [18]. We speculated that miR-204-3p/IGFBP-2 was involved in the NSCLC progression according to the reported evidence. In the current study, we proved that PART-1 targeted miR-204-3p directly, and miR-204-3p directly targeted IGFBP-2 in NSCLC cells. Furthermore, we demonstrated that PART-1 targeted miR-204-3p/IGFBP-2 pathway to regulate the NSCLC progression.

2. Materials and Methods

2.1. Cell lines

Human NSCLC cell lines, including A549, H1299, H1650, H 1975, and PC9, and the human bronchial epithelial (HBE) cell line were purchased from the National Collection of Authenticated Cell Cultures. The cell lines were cultured in Dulbecco's modified eagle medium (DMEM, Sigma-Aldrich, St. Louis, MO, USA) supplemented with 10% fetal bovine serum, non-essential amino acids, and 1% v/v Penicillin/Streptomycin (PS, Invitrogen, Carlsbad, CA, USA) at 37°C in a humidified atmosphere of 5% CO_2. The cells were passaged when 80% confluent and only cells in the exponential phase and within passage were used for the experiments.

2.2. Quantitative Reverse Transcriptase PCR analysis

The expression level of mRNA was determined by quantitative RT-PCR in a LightCycler® 96 System Real-Time PCR System (Roche, USA) using Taq Pro Universal SYBR qPCR Master Mix (Q712–02, Vazyme, China). All of the primers were synthesized at Sangon Biotech (Shanghai) Co., Ltd. The primers sequences were as follows: PART-1, forward: 5′- AAG GCC GTG TCA GAA CTC AA -3′; and reverse: 5′- GTT TTC CAT CTCA GCC TGG A -3′ [10]; miR-204-3p, forward: 5′-ACA CTC CAG CTG GGG CTG GGA AGG CAA AGG G-3′ and reverse: 5′-CTC AAC TGG TGT CGT GGA-3′ [19]; IGFBP-2, forward: 5′-TGC ACA TCC CCA ACT GTG AC-3′ and reverse 5′-TGT AGA AGA GAT GAC ACT CGG G-3′ [20]; and GAPDH, forward: 5′-TGA CGC TGG GGC TGG CAT TG-3′ and reverse: 5′-GCT CTT GCT GGG GCT GGT GG-3′ [19]. GAPDH was used as an internal control for the quantification of gene targets. The thermal cycles were set as follows: 95 °C for 30 s, followed by 40 cycles of 95 °C for 15 s and 60 °C for 30 s. The PCR products were subjected to melt curve analysis to verify the specificity. Three biological replicates and three technical replicates for each biological replicate were performed for each gene. The relative expression of RNAs was calculated using the $2^{-(\Delta\Delta Ct)}$ method.

2.3. Transfection in vitro

To conduct the transfection experiments, cells were seeded into a 12-well plate at a density of 1×10^5 cells per well. After achieving 70% confluence in a well, DNA complex, which containing 4μg plasmid and 246μL Serum-Free medium (SFM) were transfected

Preprints (www.preprints.org) | NOT PEER-REVIEWED | Posted: 24 May 2022 doi:10.20944/preprints202205.0336.v1

with lipofectamine 2000 (Invitrogen, Shanghai, China) according to the manufacturer's instructions. After 24 hours of incubation, cells were lysed for further study.

2.4. Cell viability assay

The viability of A549 cells was measured using a Cell Counting Kit-8 assay (CCK-8) kit (AbMole BioScience, Shanghai, China). Cells (1×10^3 cells/well) were seeded in 96-well plates, grown for 24 h, 48 h, 72 h, and 96 h, respectively, and then added10 μl of CCK-8 solution to the wells following incubation for 4 h. The absorbance at 450 nm was measured on a microplate reader (Model 680 microplate reader, Bio-Rad Laboratories). Triplicate wells were set for each sample, and the experiments were repeated three times.

2.5. Cell colony formation

The transfected A549 cells were seeded in a 6-well plate with a density of 1,000 cells per well, and then the cells were covered with trypsin–EDTA solution and incubated at 37°C until they become detached. Cells were cultured with the RPMI-1640 medium for 3 weeks when colonies were formed. And then the cells were washed twice with phosphate-buffered saline (PBS) after the medium was discarded. Cells were fixed with 4% para-formaldehyde for 30 min at room temperature (RT) following the colonies were stained with 1% crystal for 5 min at room temperature. Wash the cells with water until excess dye is removed, and the number of colonies was counted. Four cell wells were set for each sample, and the experiment was repeated four times at different times.

2.6. Transwell migration assay

Plate 100 μL of transfected A459 cells solution onto the upper chamber coated with 50 μL of Matrigel atrix, and incubate for 10 minutes at 37°C and 5% CO_2 to allow the cells to settle down. After that, 600 μL of DMEM medium supplemented with 10% fetal bovine serum (FBS) was added to the lower chamber. After incubating for 48 h, cells that invaded through the membrane were fixed with 4% paraformaldehyde, and then stained with 1% crystal violet for 15 min. The cell invasion was photographed under a microscope at 200× magnification (Olympus). Five fields of vision were investigated for each treatment, and average cell invasions were counted. Four cell wells were set for each sample, and the experiment was performed in triplicate.

2.7. Wound healing assay

A549 cells from each group were plated into a 6-well plate at a density of 5×10^5 cells per well. A sterile pipette tip was held vertically to scratch the cell monolayer when the cells reached 80% confluence, and the cells were washed with PBS. The serum-free medium was added to the plates, and then the plates were kept in the incubator at 37°C for 24 h. The wound closure was monitored and imaged at 0 h and 24 h using a microscope (Olympus). The migration rate= (wound width at 0 h - wound width at 24 h)/ wound width at 0 h × 100%. This experiment was conducted in triplicate for each group.

2.8. Xenograft tumor experiment

A total of 10 BALB/c nude mice were randomly and blindly divided into two groups (N = 5 per group). A549 cells transfected stably with sh-PART1 or sh-NC were harvested, and then 1×10^7 cells were inoculated subcutaneously into the axilla of nude mice to generate an A549 tumor mouse model. The tumor volumes were monitored every 3 days from the sixth day after inoculating and calculated using the following formula: volume = $0.5 \times \text{length} \times \text{width}^2$. After three weeks of treatment, the mice were euthanized to excise tumors, and the tumors were weighed.

2.9. Luciferase reporter assay

The wild-type (WT) or mutant (MT) 3′-UTR of miR-204-3p containing the putative binding sites of PART-1 was inserted into the pmiR-GLO vector. A549 cells were co-transfected with pcDNA-EGFP-pre-PART1 and pmir-GLO-PART1-miR-204-3p 3′-UTR in the presence of a luciferase reporter vector. In addition, the wild-type (WT) or mutant (MT) 3′-UTR of IGFBP containing the putative binding sites of PART-1 was inserted into the pmiR-GLO vector. A549 cells were co-transfected with pcDNA-EGFP-pre-miR-204-3p and pmir-GLO-miR-204-3p-IGFBP2 3′-UTR in the presence of a luciferase reporter vector. The cells were harvested after 48 h transfecting, and the luciferase activity was determined

Preprints (www.preprints.org) | NOT PEER-REVIEWED | Posted: 24 May 2022 doi:10.20944/preprints202205.0336.v1

with the dual-luciferase reporter system (Promega, Madison, WI, USA). The experiment was conducted in triplicate.

2.10. Western blot

Protein was extracted from the A549 cells with the RAPI lysis buffer (Solarbio, Beijing, China). The protein concentration was evaluated using the bicinchoninic acid (BCA) assay kit (Beyotime, Shanghai, China); Loading 15 μg of proteins in each well and separated by the 15% SDS-PAGE, and then transferred the proteins onto the polyvinylidene difluoride (PVDF) membrane (Millipore, Braunschweig, Germany). The membrane was firstly blocked with 5% non-fat milk at RT for 1 h, followed by incubation with primary antibodies at RT for 2 h and by incubation of the membrane with goat anti-rabbit IgG secondary antibody (1:3,000, Bio-Rad, CA, USA). ECL imaging system was used for imaging, and ImageJ software was used to quantify the intensities of protein bands (https://imagej.nih.gov/ij/). GAPDH was used as the loading control.

2.11. Statistical analysis

Results were presented as mean ± standard deviation from three independent experiments. The data were analyzed with the SPSS 19.0 software (SPSS Inc., Chicago, IL, USA). Significant differences between/among treatment groups were analyzed using unpaired Student's t-test or one-way ANOVA followed by Dunnett's post hoc test. $P < 0.05$ was considered to be statistically significant.

3. Results

3.1. PART-1 was up-regulated in the NSCLC Cell Lines

We detected the expression level of prostate androgen-regulated transcript 1 (*PART-1*) in the human bronchial epithelial (HBE) cell line, and the human non-small cell lung cancer (NSCLC) cell lines, including A549, H1229, H1650, H1975, and PC9, by quantitative RT-PCR. The expression level of the PART-1 gene increased significantly in the NSCLC cell lines (Fig.1, $P<0.05$). The expression levels were 3.15, 2.78, 2.24, 1.9, and 1.71 times that in HBE cells, respectively (Fig.1).

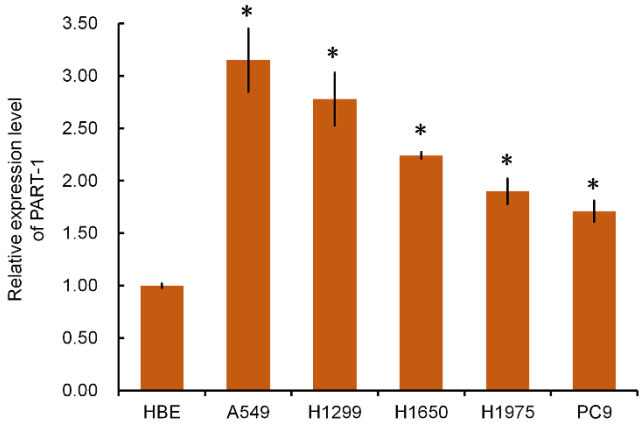

Figure 1. The expression of PART-1 in the HBE cell line, and the NSCLC cell lines, including A549, H1229, H1650, H1975, and PC9, by quantitative RT-PCR. The expression level of the PART-1 gene increased significantly in the NSCLC cell lines. *: indicates $P<0.05$.

3.2. Knocking down of PART-1 inhibited the proliferation, invasion, and migration of A549 cells

We knocked down the PART-1 by lentiviral shRNA and achieved two types of A549 cells: cells with silenced PART-1 (sh-PART1 group), and cells transfected with a non-coding shRNA (sh-NC group). The expression level of PART-1 in sh-PART1 cells was decreased to 0.557 times that in sh-NC cells by RT-PCR (Fig2A).

The proliferation of transfected A549 cells was measured by the CCK-8 kit. The transfected cells were selected by puromycin and then monitored continuously for 96 h. The OD values of sh-PART1 cells and sh-NC cells increased with time, however, the value of sh-NC cells increased faster than that of sh-PART1 cells, and the OD values of sh-PART1

Preprints (www.preprints.org) | NOT PEER-REVIEWED | Posted: 24 May 2022 doi:10.20944/preprints202205.0336.v1

cells were significantly lower than that of sh-NC cells after 96 incubation (Fig.2B). The results demonstrated that proliferation of A549 cells was inhibited by the down-regulated of PART-1. The average number of cell colonies were 110 and 265 formed by sh-PART1 cells and sh-NC cells, respectively, by colony formation assays (Fig.2C). sh-PART1 cells had significantly decreased numbers of cell colonies compared with that sh-NC cells (Fig.2C, $P<0.05$). The cell invasion was detected by Transwell invasion assay. The average number of cells invaded were 82 and 138 for sh-PART1 cells and sh-NC cells, respectively, which means the cell invasion was inhibited by down-regulated PART-1 (Fig.2D $P<0.05$). The migration of A549 cells was tested by wound healing assay. The results showed that the migration was significantly reduced by down-regulated PART-1 of sh-PART1 cells compared with that of sh-NC cells (Fig. 2E).

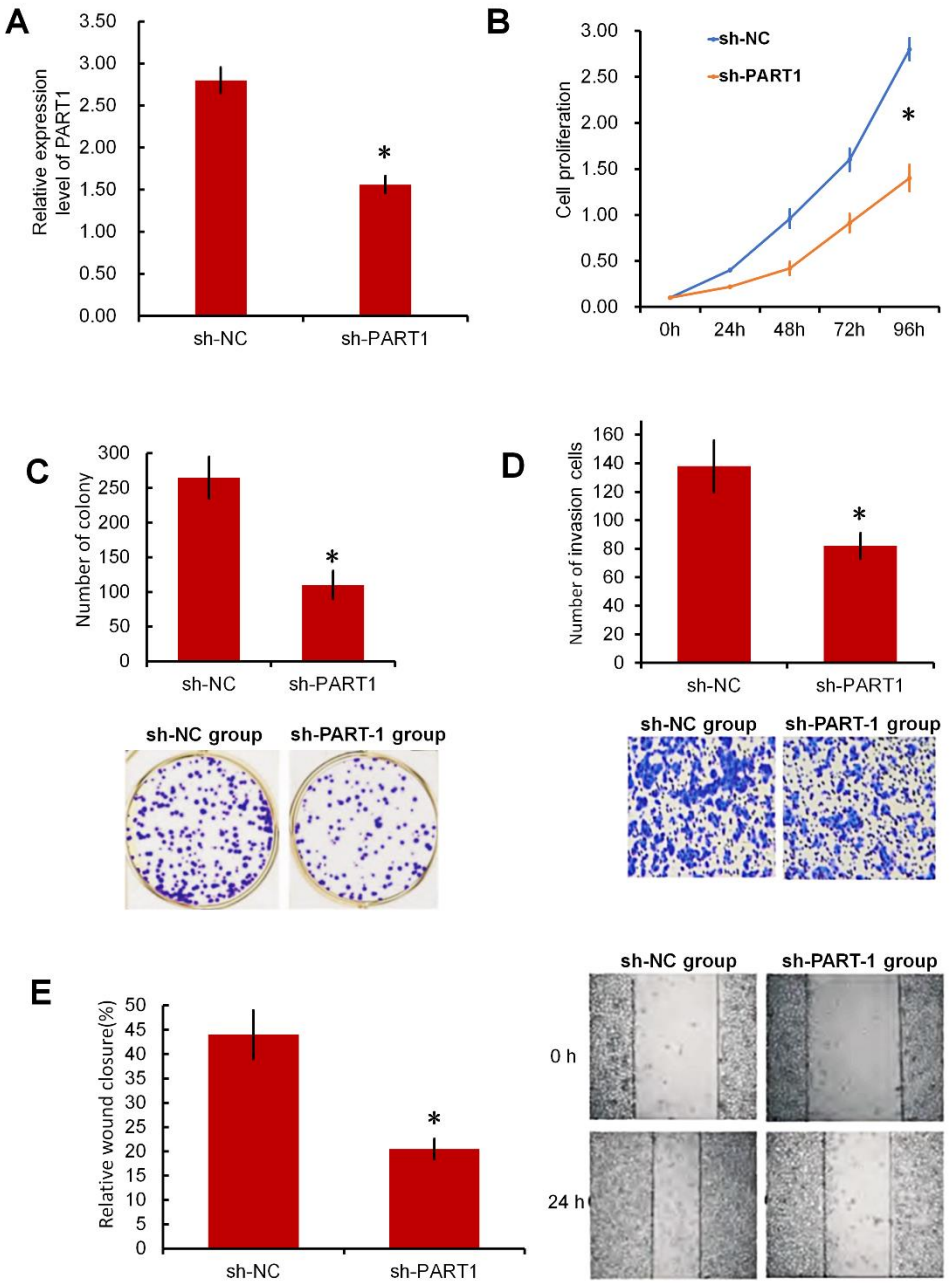

Figure 2. The effect of knocking down PART-1 on the proliferation, invasion, and migration of A549 cells. (A) The expression of PART-1 in A549 cells with the transfection of PART-1 shRNAs and negative control were validated by RT-qPCR. (B) The proliferation of cells of sh-PART1 and sh-NC was determined by the CCK-8 assay. (C) Colony formation of sh-PART1 and sh-NC cells. (D, E) The cell invasion and wound healing results of sh-PART1 and sh-NC cells by Transwell invasion assay and wound healing assay. *$P<0.05$ sh-PART1 group vs. sh-NC group.

Preprints (www.preprints.org) | NOT PEER-REVIEWED | Posted: 24 May 2022 doi:10.20944/preprints202205.0336.v1

3.3. The development of tumor was inhibited by down-regulated PART-1 in nude mice

An A549 tumor mouse model was generated to demonstrate the function of PART-1 on the development of tumors. The A549 cells of the sh-PART1 and sh-NC group were inoculated to the axilla of nude mice, respectively, and the growth of the tumor was monitored. The size of tumors was measured once every three days from 6 days after inoculation, the results showed that the volume of tumors increased along with the time (Fig. 3A). The tumors were excised and weighed three weeks after injecting, the tumor weight of the sh-PART1 group was 0.101 g, which was significantly lighter than that of the sh-NC group (0.221 g) (Fig. 3B and 3C). The inhibitory rate of tumor growth was 54.30% by the down-regulation of PART-1.

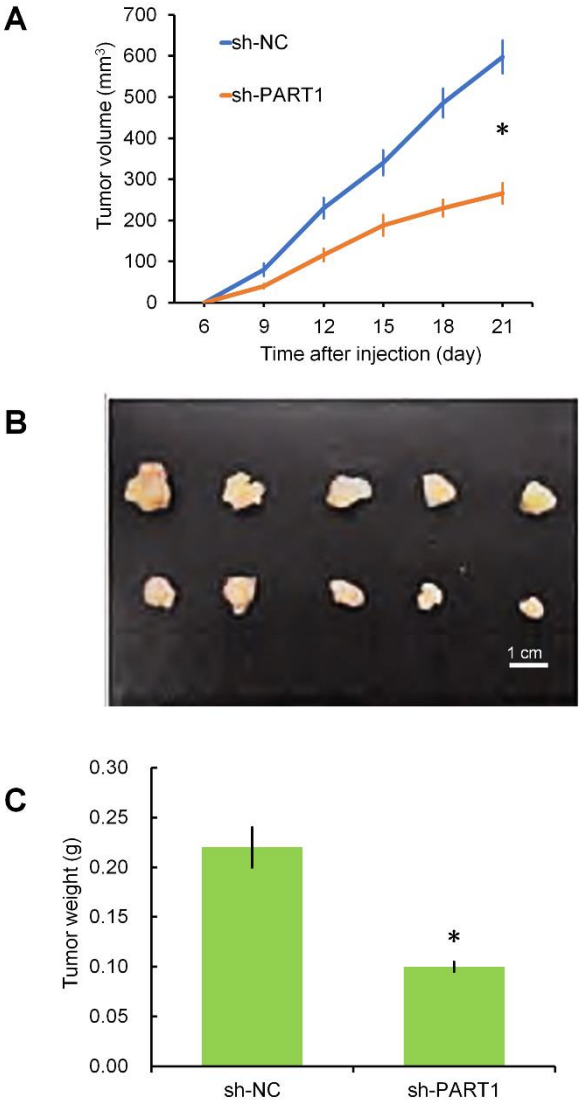

Figure 3. Down-regulation of PART-1 reduced NSCLC tumor growth in vivo. sh-PART1 and sh-NC cells were inoculated into nude mice (n=5 per group) at 1 × 107 per mouse subcutaneously. (A) Tumor volume from 6 to 21 days after inoculating. (B, C) The tumors that were excised from mice at 21 days after inoculation, and average tumor weight. *P<0.05 sh-PART1 group vs. sh-NC group.

3.4. PART-1 targeted MiR-204-3p, and negatively regulated the expression of IGFBP-2

To further explore the underlying molecular mechanism by which PART-1 modulated the growth of A549 cells, the targets of PART-1 were predicted using the starBase v2.0 [21], and miR-204-3p was predicted as a possible target of PART-1. In addition, insulin-like growth factor binding protein 2 (IGFBP-2) was reported previously as a target of miR-204-3p [17]. We confirmed the binding between PART-1 with the miR-204-3p and miR-204-3p with the IGFBP-2. The WT or MT 3′-UTR of PART-1 containing the putative

Preprints (www.preprints.org) | NOT PEER-REVIEWED | Posted: 24 May 2022 doi:10.20944/preprints202205.0336.v1

binding sites of miR-204-3p was inserted into the pmiR-GLO vector. Luciferase reporter assay was performed by co-transfecting negative control miRNA or miR-204-3p mimics with WT or MT 3′-UTR of PART-1. The results showed that overexpression of WT 3′-UTR of PART-1 significantly reduced the luciferase activity of the miR-204-3p; however, no remarkable decrease was observed when cells were transfected with MUT 3′-UTR of PART-1 (Figures 4A). Meanwhile, the expression level of miR-204-3p increased significantly in the sh-PART1 cells compared with that in sh-NC cells by RT-qPCR assay. Those results indicated that the 3′-UTR of PART-1 bound miR-204-3p directly.

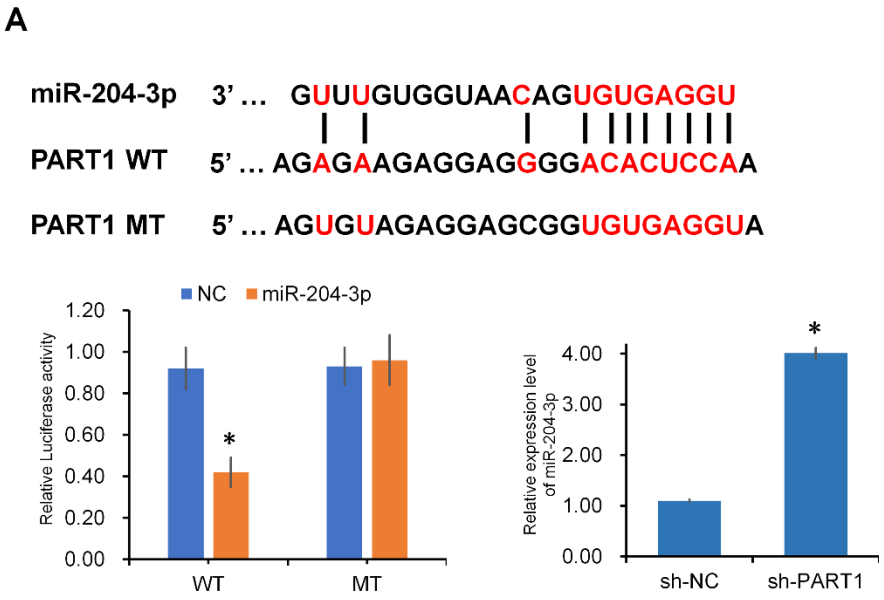

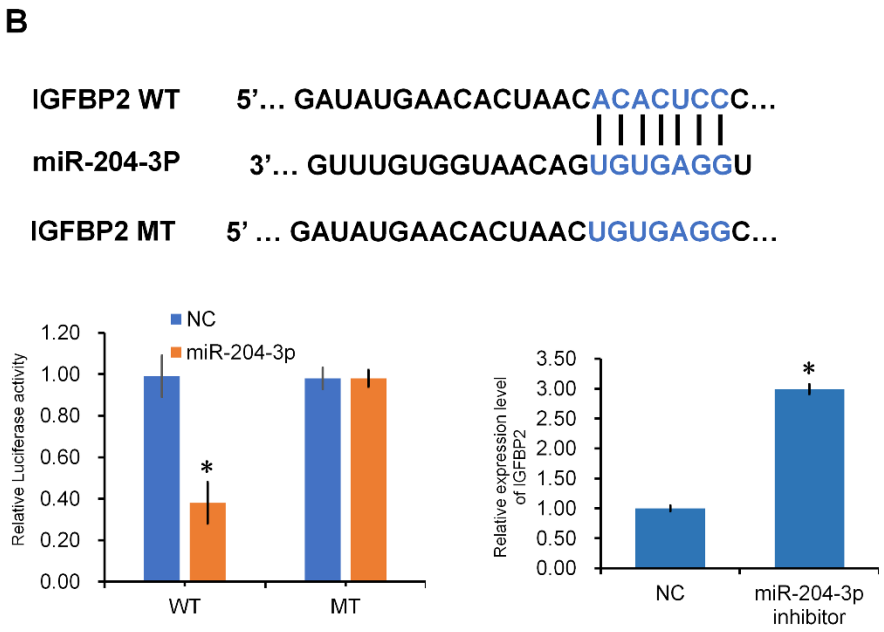

Figure 4. Confirmation of PART-1 targeted miR-204-3p and miR-204-3p targeted IGFBP-2. (A) Potential binding site between PART-1 with miR-204-3p and dual-luciferase reports indicated the interaction between PART-1 and miR-204-3p. The relative expression level of miR-204-3p in sh-PART1 cells compared with that in sh-NC cells. (B) The potential binding site between miR-204-3p with IGFBP-2 and dual-luciferase reports indicated the interaction between miR-204-3p and IGFBP-2. The relative expression level of IGFBP-2 in miR-204-3p inhibited cells compared with that in negative control cells. * Indicates the $P<0.05$.

Preprints (www.preprints.org) | NOT PEER-REVIEWED | Posted: 24 May 2022 doi:10.20944/preprints202205.0336.v1

Overexpression of WT 3′-UTR of IGFBP-2 significantly reduced the luciferase activity of the miR-204-3p, but no remarkable decrease while overexpressing MT 3′-UTR of IGFBP-2 (Figures 4B). Furthermore, the expression level increased when the miR-204-3p was inhibited in A549 cells (Figures 4B). The results indicated that miR-204-3p targeted the 3′-UTR IGFBP-2 directly.

3.5. Knocking down of PART-1 inhibited the proliferation, invasion, and migration of A549 cells by regulating the miR-204-3p-targeted IGFBP-2 pathway

The expression level of IGFBP-2 mRNA and protein was remarkably inhibited via RT-qPCR assay and western blot in PART-1 down-regulated A549 cells (P<0.05, Fig.5). Meanwhile, the expression level partly recovered by transfecting the PART1-shRNA + miR204-3p inhibitor or PART1-shRNA + IGFBP2 over-expression vectors (P<0.05, Fig.5).

We performed serial experiments to demonstrate the knock-down of PART-1 affects the proliferation, invasion, and migration of A549 cells by the miR-204-3p-targeted IGFBP-2 pathway. The inhibits of proliferation, invasion, and migration were partly recovered in PART-1 knocked-down A549 cells via down-regulated miR-204-3p or overexpressed IGFBP-2 (P<0.05, Fig. 6).

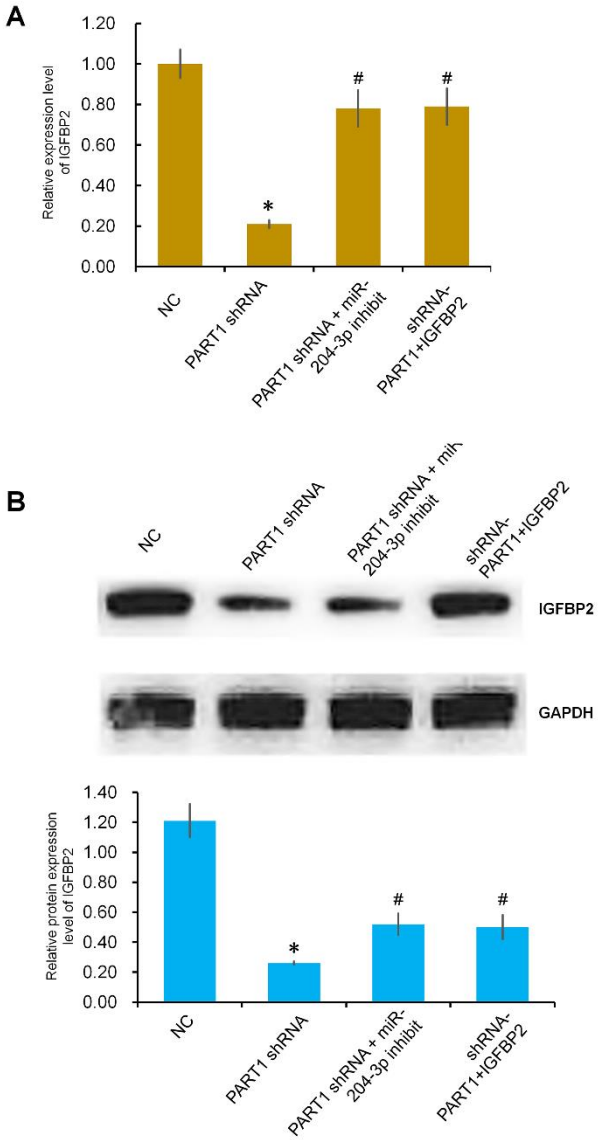

Figure 5. Effect of PART-1 and miR-204-3p on the expression of IGFBP-2 in NC, PART1-shRNA, PART1-shRNA + miR204-3p inhibitor, and PART1-shRNA + IGFBP2 group, respectively. (A) The relative expression level of mRNA of IGFBP-2 by quantitative RT-PCR. (B) The expression protein level of IGFBP-2 by western blot. GAPDH was used as internal

Preprints (www.preprints.org) | NOT PEER-REVIEWED | Posted: 24 May 2022 doi:10.20944/preprints202205.0336.v1

controls; * PART1-shRNA group comparing with NC group, P<0.05; # comparing with PART1-shRNA group, P<0.05.

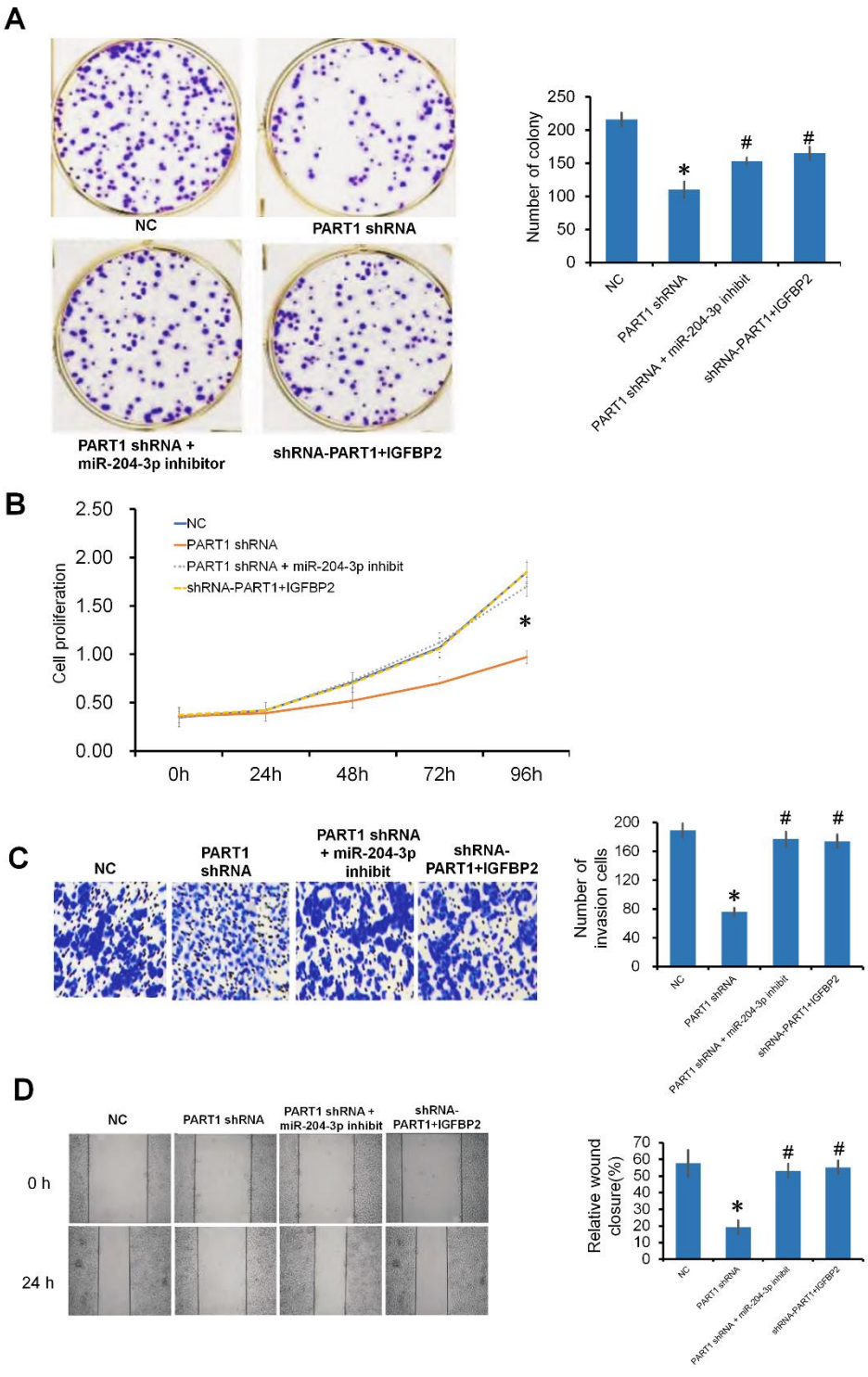

Figure 6. The down-regulate of PART1 inhibited the proliferation, invasion, and migration of A549 cells by regulating the miR-204-3p-targeted IGFBP-2 pathway. (A) Colony formation of NC, PART1-shRNA, PART1-shRNA + miR204-3p inhibitor, and PART1-shRNA + IGFBP2 cells. (B) The proliferation of cells that determined by the CCK-8 assay. (C, D) The cell invasion and wound healing results of NC, PART1-shRNA, PART1-shRNA + miR204-3p inhibitor, and PART1-shRNA + IGFBP2 cells by Transwell invasion assay and wound healing assay. * * PART1-shRNA group compared with NC group, P<0.05; # comparing with PART1-shRNA group, P<0.05.

 doi:10.20944/preprints202205.0336.v1

4. Discussion

The vast majority (85 percent) of lung cancers fall into the category called non-small cell lung cancer (NSCLC). Though this form of lung cancer progresses more slowly than SCLC, 40 percent of NSCLCs will have spread beyond the lungs by the time it is diagnosed [3]. Making the pathogenesis of NSCLC clear is valuable to control the disease [22]. LncRNAs promote cancer cell growth and development by targeting miRNAs [23]. PART-1 (prostate androgen-regulated transcript 1) that maps to chromosome 5q12 is predominantly expressed in the prostate and is regulated by androgens in human prostate cancer cells [24]. Moreover, PART-1 was reported that promote the development of several cancers, such as breast cancer, cervical squamous cell carcinoma, and glioma [17,25,26]. The role of PART-1 on the progression of NSCLC was not clear till now. In the current study, we found that the expression of PART-1 in A549, H1229, H1650, H1975, and PC9 cells were significantly increased compared with that in HBE cells. Repeated results were achieved in NSCLC cells, including A549, H1229, H1650, SKMES-1, and H1975. We concluded that PART-1 may promote the development of NSCLC, and conducted serial experiments to prove the hypothesis.

We knocked down the PART-1 from A549 cells and found that the down-regulate PART-1 inhibited the proliferation, invasion, and migration of A549 cells. Furthermore, the growth of tumor was inhibited when PART-1 was knocked down in the mice tumor models. Those results confirmed that PART-1 regulated the NSCLC progression. PART-1 took part in the tumor progression via a wide variety of mechanisms. PART-1 modulated toll-like receptor pathways to influence prostate cancer development [27]. However, more reports demonstrated that PART-1 functions in cancer development by regulating networks among circRNA/miRNA/mRNA. PART-1 regulates colorectal cancer via targeting miR-150-5p/miR-520h/CTNNB1, and promotes breast cancer cell progression by directly targeting miR-4516 [11,25].

To explore further the mechanism of PART-1 promoting the development of NSCLC, we searched the target miRNA of PART-1, and miR-204-3p was predicted as a possible target of PART-1. In addition, miR-204-3p targeted insulin-like growth factor binding protein 2 (IGFBP-2) directly and is involved in the development of glioma [17]. We confirmed the targets among PART-1, miR-204-3p, and IGFBP-2 by luciferase reporter assay in the current study. The expression of miR-204-3p inhibited the development of cancers. The IGFBP-2/AKT/Bcl2 pathway via miR-204-3p targeting played a critical role in mediating glioma cell death [17]. IGFBP-2 is involved in the NSCLC progression, and the expression of IGFBP-2 in lung cancer patients was significantly higher than that in controls and increased with lung cancer progressed to an advanced stage [28]. In the current study, expression of mRNA and protein of IGFBP-2 both increased after transfecting the PART1-shRNA + miR204-3p inhibitor or PART1-shRNA + IGFBP2 over-expression vectors, which were remarkably higher than that in sh-PART1 cells. The proliferation, invasion, and migration were inhibited by knocking down of PART-1, and the inhibition of PART-1 was partly recovered by the down-regulation of miR204-3p or overexpression of IGFBP-2. Combining the results achieved in the current study, we conclude that PART-1 inhibited proliferation, invasion, and migration of NSCLC via up-regulating miR204-3p/ IGFBP-2. PART-1 might be a target for treating NSCLC, however, the relationship between expression of PART-1 and clinicopathological features and prognosis of NSCLC needs to be further explored. In addition, PART-1 might be a warning sign of diagnosis of early lung cancer.

Author Contributions: Conceptualization, K.F.L., L.S., X.H. D. and Y.P.Z.; methodology, K.F.L., X.G. and Y.F.W.; validation, K.F.L., Y.P.Z. ,Y.F.W. and X.G.; formal analysis, K.F.L.; investigation, Y.P.Z. , X.H.D. and L.S.; resources, K.F.L.; data curation, K.F.L., Y.F.W. and L.S.; writing—original draft preparation, K.F.L., L.S.,Y.G. and Y.F.W.; writing—review and editing, K.F.L., Y.P.Z., Y.F.W., Y.G., X.H. D. and L.S.; visualization, K.F.L.; supervision, K.F.L. and L.S.; project administration, K.F.L. and L.S. All authors have read and agreed to the published version of the manuscript.

Funding: This research received no external funding.

Institutional Review Board Statement: The study was conducted in accordance with the Declaration of Helsinki, and approved by the Institutional Animal Care and Use Committee (IACUC) of Chengyang People Hospital (IACUC:2017082600). Approval Date: 26 August 2017.

Informed Consent Statement: Informed consent was obtained from all subjects involved in the study.

Data Availability Statement: The data presented in this study are available on request from the corresponding author.

Acknowledgments: The authors would like to express special thanks of gratitude to Dr. Sen Lian at Qingdao Agricultural University for his technical support to the study.

Conflicts of Interest: The authors declare no conflict of interest.

References

1. Gridelli, C.; Rossi, A.; Carbone, D.P.; Guarize, J.; Karachaliou, N.; Mok, T.; Petrella, F.; Spaggiari, L.; Rosell, R. Non-small-cell lung cancer. *Nat. Rev. Dis. Primers* **2015**, *1*, 15009, doi:10.1038/nrdp.2015.9.
2. Barta, J.A.; Powell, C.A.; Wisnivesky, J.P. Global epidemiology of lung cancer. *Ann. Glob. Health* **2019**, *85*, doi:10.5334/aogh.2419.
3. Bade, B.C.; Dela Cruz, C.S. Lung Cancer 2020: Epidemiology, etiology, and prevention. *Clin. Chest Med.* **2020**, *41*, 1-24, doi:10.1016/j.ccm.2019.10.001.
4. Xie, S.; Wu, Z.; Qi, Y.; Wu, B.; Zhu, X. The metastasizing mechanisms of lung cancer: Recent advances and therapeutic challenges. *Biomed. Pharmacotherapy* **2021**, *138*, 111450, doi:https://doi.org/10.1016/j.biopha.2021.111450.
5. Schegoleva, A.A.; Khozyainova, A.A.; Fedorov, A.A.; Gerashchenko, T.S.; Rodionov, E.O.; Topolnitsky, E.B.; Shefer, N.A.; Pankova, O.V.; Durova, A.A.; Zavyalova, M.V.; et al. Prognosis of different types of non-small cell lung cancer progression: Current state and perspectives. *Cell Physiol. Biochem.* **2021**, *55*, 29-48, doi:10.33594/000000340.
6. Quinn, J.J.; Chang, H.Y. Unique features of long non-coding RNA biogenesis and function. *Nat. Rev. Genet.* **2016**, *17*, 47-62, doi:10.1038/nrg.2015.10.
7. He, Q.; Long, J.; Yin, Y.; Li, Y.; Lei, X.; Li, Z.; Zhu, W. Emerging roles of lncRNAs in the formation and progression of Colorectal cancer. *Front. Oncol.* **2020**, *9*, 1542-1542, doi:10.3389/fonc.2019.01542.
8. Zhang, Y.; Xu, Y.; Feng, L.; Li, F.; Sun, Z.; Wu, T.; Shi, X.; Li, J.; Li, X. Comprehensive characterization of lncRNA-mRNA related ceRNA network across 12 major cancers. *Oncotarget* **2016**, *7*, 64148-64167, doi:10.18632/oncotarget.11637.
9. Sidiropoulos, M.; Chang, A.; Jung, K.; Diamandis, E.P. Expression and regulation of prostate androgen regulated transcript-1 (PART-1) and identification of differential expression in prostatic cancer. *Br. J. Cancer* **2001**, *85*, 393-397, doi:10.1054/bjoc.2001.1883.
10. Pan, Z.; Mo, F.; Liu, H.; Zeng, J.; Huang, K.; Huang, S.; Cao, Z.; Xu, X.; Xu, J.; Liu, T.; et al. LncRNA prostate androgen-regulated transcript 1 (PART 1) functions as an oncogene in osteosarcoma via sponging miR-20b-5p to upregulate BAMBI. *Ann. Transl. Med.* **2021**, *9*, 488, doi:10.21037/atm-21-658.
11. Zhou, T.; Wu, L.; Ma, N.; Tang, F.; Zong, Z.; Chen, S. LncRNA PART1 regulates colorectal cancer via targeting miR-150-5p/miR-520h/CTNNB1 and activating Wnt/β-catenin pathway. *Int. J. Biochem. Cell Biol.* **2020**, *118*, 105637, doi:10.1016/j.biocel.2019.105637.
12. Mohr, A.M.; Mott, J.L. Overview of microRNA biology. *Semin. Liver Dis.* **2015**, *35*, 3-11, doi:10.1055/s-0034-1397344.
13. Kwak, P.B.; Iwasaki, S.; Tomari, Y. The microRNA pathway and cancer. *Cancer Sci.* **2010**, *101*, 2309-2315, doi:10.1111/j.1349-7006.2010.01683.x.
14. Farazi, T.A.; Spitzer, J.I.; Morozov, P.; Tuschl, T. miRNAs in human cancer. *J. Pathol.* **2011**, *223*, 102-115, doi:10.1002/path.2806.

15. Han, Z.; Zhang, Y.; Sun, Y.; Chen, J.; Chang, C.; Wang, X.; Yeh, S. ERβ-mediated alteration of circATP2B1 and miR-204-3p signaling promotes invasion of Clear Cell Renal Cell Carcinoma. *Cancer Res.* **2018**, *78*, 2550-2563, doi:10.1158/0008-5472.Can-17-1575.
16. Guo, J.; Zhao, P.; Liu, Z.; Li, Z.; Yuan, Y.; Zhang, X.; Yu, Z.; Fang, J.; Xiao, K. MiR-204-3p inhibited the proliferation of Bladder cancer cells via modulating lactate Dehydrogenase-mediated glycolysis. *Front. Oncol.* **2019**, *9*, 1242-1242, doi:10.3389/fonc.2019.01242.
17. Chen, P.H.; Chang, C.K.; Shih, C.M.; Cheng, C.H.; Lin, C.W.; Lee, C.C.; Liu, A.J.; Ho, K.H.; Chen, K.C. The miR-204-3p-targeted IGFBP2 pathway is involved in xanthohumol-induced glioma cell apoptotic death. *Neuropharmacology* **2016**, *110*, 362-375, doi:10.1016/j.neuropharm.2016.07.038.
18. Dong, J.; Zeng, Y.; Zhang, P.; Li, C.; Chen, Y.; Li, Y.; Wang, K. Serum IGFBP2 level is a new candidate biomarker of severe malnutrition in advanced lung cancer. *Nutr. Cancer* **2020**, *72*, 858-863, doi:10.1080/01635581.2019.1656755.
19. Liu, W.; Li, X.; Tan, X.; Huang, X.; Tian, B. MicroRNA-204-3p inhibits metastasis of pancreatic cancer via downregulating MGAT1. *J. BUON.* **2021**, *26*, 2149-2156.
20. Lee, C.-C.; Chen, P.-H.; Ho, K.-H.; Shih, C.-M.; Cheng, C.-H.; Lin, C.-W.; Cheng, K.-T.; Liu, A.-J.; Chen, K.-C. The microRNA-302b-inhibited insulin-like growth factor-binding protein 2 signaling pathway induces glioma cell apoptosis by targeting nuclear factor IA. *PloS One* **2017**, *12*, e0173890-e0173890, doi:10.1371/journal.pone.0173890.
21. Li, J.H.; Liu, S.; Zhou, H.; Qu, L.H.; Yang, J.H. starBase v2.0: decoding miRNA-ceRNA, miRNA-ncRNA and protein-RNA interaction networks from large-scale CLIP-Seq data. *Nucleic Acids Res.* **2014**, *42*, D92-97, doi:10.1093/nar/gkt1248.
22. Tang, X.J.; Wang, W.; Hann, S.S. Interactions among lncRNAs, miRNAs and mRNA in colorectal cancer. *Biochimie* **2019**, *163*, 58-72, doi:10.1016/j.biochi.2019.05.010.
23. Seo, D.; Kim, D.; Chae, Y.; Kim, W. The ceRNA network of lncRNA and miRNA in lung cancer. *Genomics Inform.* **2020**, *18*, e36-e36, doi:10.5808/GI.2020.18.4.e36.
24. Lin, B.; White, J.T.; Ferguson, C.; Bumgarner, R.; Friedman, C.; Trask, B.; Ellis, W.; Lange, P.; Hood, L.; Nelson, P.S. PART-1: a novel human prostate-specific, androgen-regulated gene that maps to chromosome 5q12. *Cancer Res.* **2000**, *60*, 858-863.
25. Wang, Z.; Xu, R. lncRNA PART1 Promotes Breast Cancer Cell Progression by Directly Targeting miR-4516. *Cancer Manag. Res.* **2020**, *12*, 7753-7760, doi:10.2147/CMAR.S249296.
26. Liu, H.; Zhu, C.; Xu, Z.; Wang, J.; Qian, L.; Zhou, Q.; Shen, Z.; Zhao, W.; Xiao, W.; Chen, L.; et al. lncRNA PART1 and MIR17HG as ΔNp63α direct targets regulate tumor progression of cervical squamous cell carcinoma. *Cancer Sci.* **2020**, *111*, 4129-4141, doi:https://doi.org/10.1111/cas.14649.
27. Sun, M.; Geng, D.; Li, S.; Chen, Z.; Zhao, W. LncRNA PART1 modulates toll-like receptor pathways to influence cell proliferation and apoptosis in prostate cancer cells. *Biol. Chem.* **2018**, *399*, 387-395, doi:10.1515/hsz-2017-0255.
28. Tang, D.; Yao, R.; Zhao, D.; Zhou, L.; Wu, Y.; Yang, Y.; Sun, Y.; Lu, L.; Gao, W. Trichostatin A reverses the chemoresistance of lung cancer with high IGFBP2 expression through enhancing autophagy. *Sci. Rep.* **2018**, *8*, 3917, doi:10.1038/s41598-018-22257-1.